Hybrid Simulation of Global Alfvén Eigenmode and Energetic Particle Mode in Heliotron J, a Low Shear Helical Axis Heliotron

ID#78

P. Adulsiriswad[1], Y. Todo[2], S. Yamamoto[3], S. Kado[4], S. Kobayashi[4], S.Ohshima[4], H. Okada[4], T. Minami[4]
Y. Nakamura[1], A. Ishizawa[1], T. Mizuuchi[4], S. Konoshima[4], K. Nagasaki[4],

1. Graduate School of Energy Science, Kyoto University, Uji, 611-0011 Japan,
2. National Institute for Fusion Science, Toki, Gifu 509-5292, Japan
3. Naka Fusion Institute, National Institutes for Quantum and Radiological Science and Technology,
4. Institute of Advanced Energy, Kyoto University, Uji, 611-011, Japan

I. Research Background & Objectives

- Understanding the **interplay** between energetic particle and MHD wave (Energetic particle driven mode) is important to achievement a self-sustainable fusion plasma.
- MEGA[1] code solves time evolution of energetic particle-driven mode in real space.
  → Successfully apply to Tokamak and planar axis stellarator/heliotron (LHD).
- Objective of this study is to **apply** MEGA code to study EP-driven mode in advanced stellarator/heliotron configuration (Heliotron J).
  1. *Clarify the interplay between the energetic particle and MHD wave in low equilibrium field period stellarator.*
  2. *Demonstrate nonlinear hybrid simulation in helical axis stellarator/heliotron.*

II. Numerical Model : MEGA[1]

- Hybrid simulation model, where bulk plasma and energetic particle are presented by full MHD equations and drift kinetic equations, respectively.

A. Full MHD Equations

(1) $\frac{\partial \rho}{\partial t} + \nabla \cdot (\rho \vec{v}) + \nu \nabla^2 (\rho - \rho_{eq}) = 0$

(2) $\rho \left[\frac{\partial \vec{v}}{\partial t} + (\vec{v} \cdot \nabla)\vec{v}\right] = \left(\frac{\nabla \times \vec{B}}{\mu_o} - \vec{J}'_\alpha\right) \times \vec{B} \ldots$
$- \nabla p - \left[\nabla \times (\upsilon \rho \nabla \times \vec{v}) + \frac{4}{3}\nabla(\upsilon \rho \nabla \cdot \vec{v})\right]$

(3) $\frac{\partial p}{\partial t} = -\nabla \cdot (p\vec{v}) - (\gamma - 1)p\nabla \cdot \vec{v} \ldots$
$+\eta\left(\frac{\nabla \times \vec{B}}{\mu_o} - \vec{J}'_\alpha\right)\delta\vec{J} + \upsilon\rho(\gamma - 1)(\nabla \times \vec{v})^2 \ldots$
$+\frac{4}{3}\upsilon\rho(\gamma - 1)(\nabla \cdot \vec{v})^2 + \chi\nabla^2 p$

(4) $\frac{\partial \vec{B}}{\partial t} = -\nabla \times \vec{E}$; (5) $\mu_o \vec{J} = \nabla \times \vec{B}$;

(6) $\vec{E} = -\vec{v} \times \vec{B} + \eta(\vec{J} - \vec{J}_{\rm eq})$

E, B →

← $\boldsymbol{J_\alpha}$

B. EP Drift Kinetic Equations

(1) $\vec{u} = \frac{v_{||}}{||B^*||}\left[\vec{B} + \left(\frac{m_\alpha v_{||}}{Z_\alpha ||B||}\right) B\nabla \times \vec{b}\right] + \frac{\vec{E} \times \vec{b}}{||B^*||} - \frac{\mu \nabla B \times \vec{b}}{Z_\alpha e ||B||}$

(2) $m_\alpha v_{||}\frac{dv_{||}}{dt} = \frac{v_{||}}{||B^*||}\left[\vec{B} + \left(\frac{m_\alpha v_{||}}{Z_\alpha ||B||}\right) B\nabla \times \vec{b}\right] \ldots \cdot \left[Z_\alpha \vec{E} - \mu \nabla B\right]$

(3) $\vec{J}'_\alpha = \int \frac{v_{ll}}{||B^*||}(\left[\vec{B} + \left(\frac{m_\alpha v_{ll}}{Z_\alpha ||B||}\right) B\nabla \times \vec{b}\right] \ldots - \frac{\mu \nabla B \times \vec{b}}{Z_\alpha e ||B^*||}) f dv^3 + \nabla \times \vec{M}$

$\vec{M} = -\int \mu \hat{b} f d^3 v,$

III. Experimentally Observed Energetic Particle-driven Mode

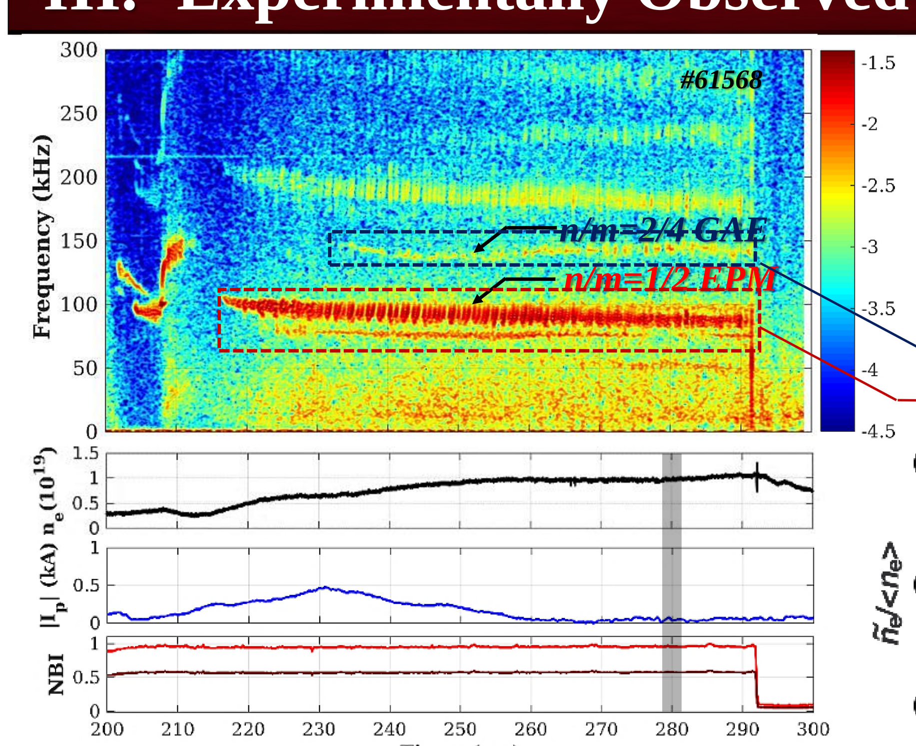

Fig. 3.1: Power spectrum density of magnetic probe signal and time evolution of plasma parameters.

- Heliotron J is a **low shear helical axis** heliotron with 4 equilibrium field period.
  → Global Alfvén eigenmode (GAE)[2,3]
  → Energetic Particle mode (EPM)[2,3]
  → Low frequency Alfvénic mode (BAE?)[4]

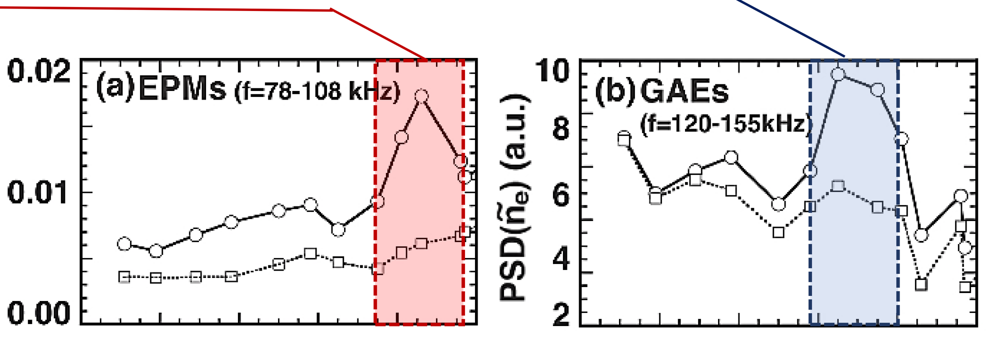

Fig. 3.2: Density fluctuation signal from BES for (a) f=78-108 kHz and (b) f=120-155 kHz

IV. MHD Equilibrium, Shear Alfvén Continua :

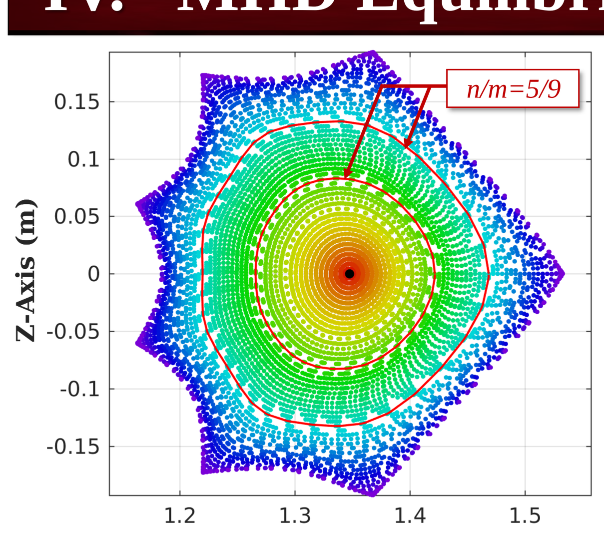

- Low bumpiness Cfg.
  - 5:3 Toroidal mirror
- Low plasma beta
  - $\beta_0 = 0.38\%$
- No net plasma current.
  - $\langle I_p \rangle \approx 0\ kA$

Fig. 4.1: Poincare plot of equilibrium magnetic field at corner section of Heliotron J

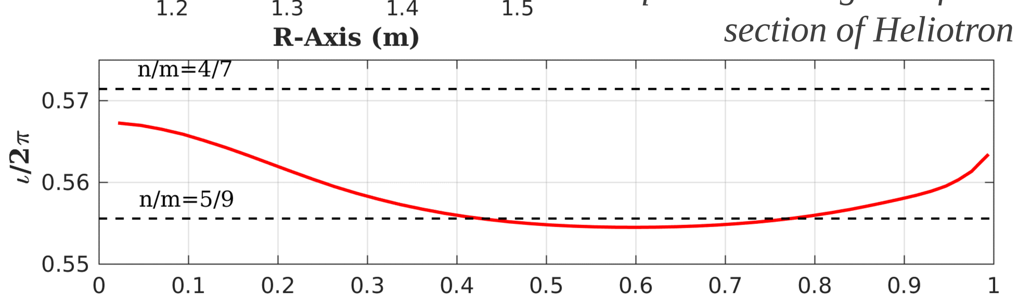

Fig. 4.2: Equilibrium rotational transform profile of the equilibrium magnetic field.

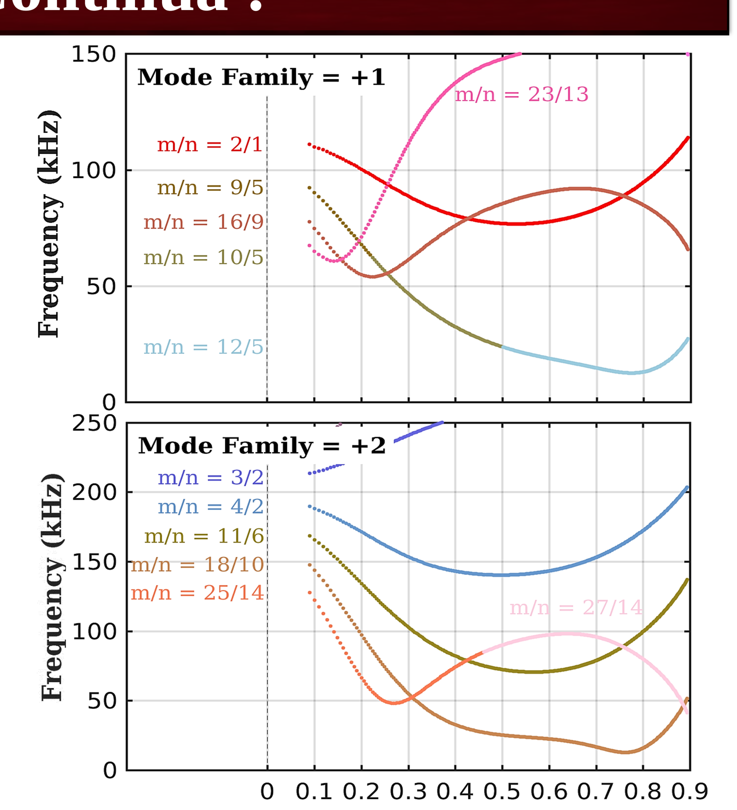

Fig. 4.3: (a) Shear Alfvén continua for n=1 and (b) n=2 toroidal mode families.

V. Equilibrium Energetic Particle Distribution :

- Bump-on-tail energy distribution is utilized due to finite charge exchange loss[5].
- Destabilization effect from spatial, **velocity** and **pitch angle** gradient are included.

$$\gamma \propto \frac{\partial f_s}{\partial \vec{r}}, \frac{\partial f_\Lambda}{\partial \Lambda}, \frac{\partial f_v}{\partial \vec{v}} \quad , \Lambda = \frac{\mu B}{E}$$

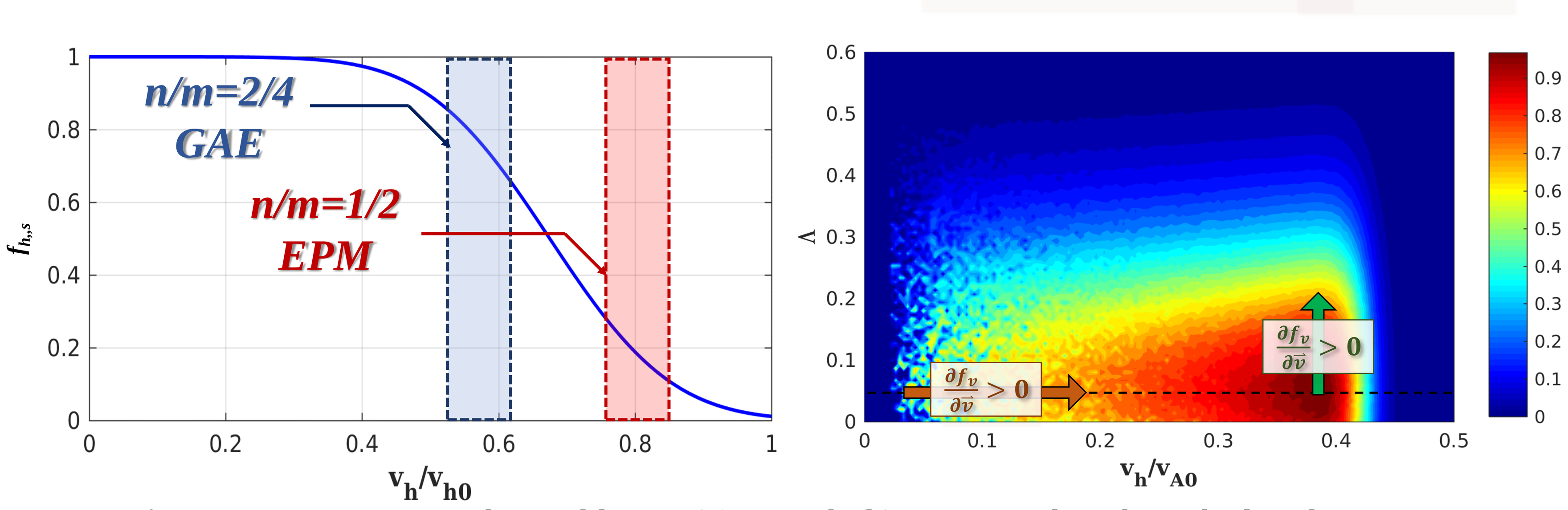

Fig. 5.1: Energetic particle equilibrium (a) spatial, (b) energy and pitch angle distributions

VI. Simulation Results

A. Observation of Global Alfvén eigenmode :

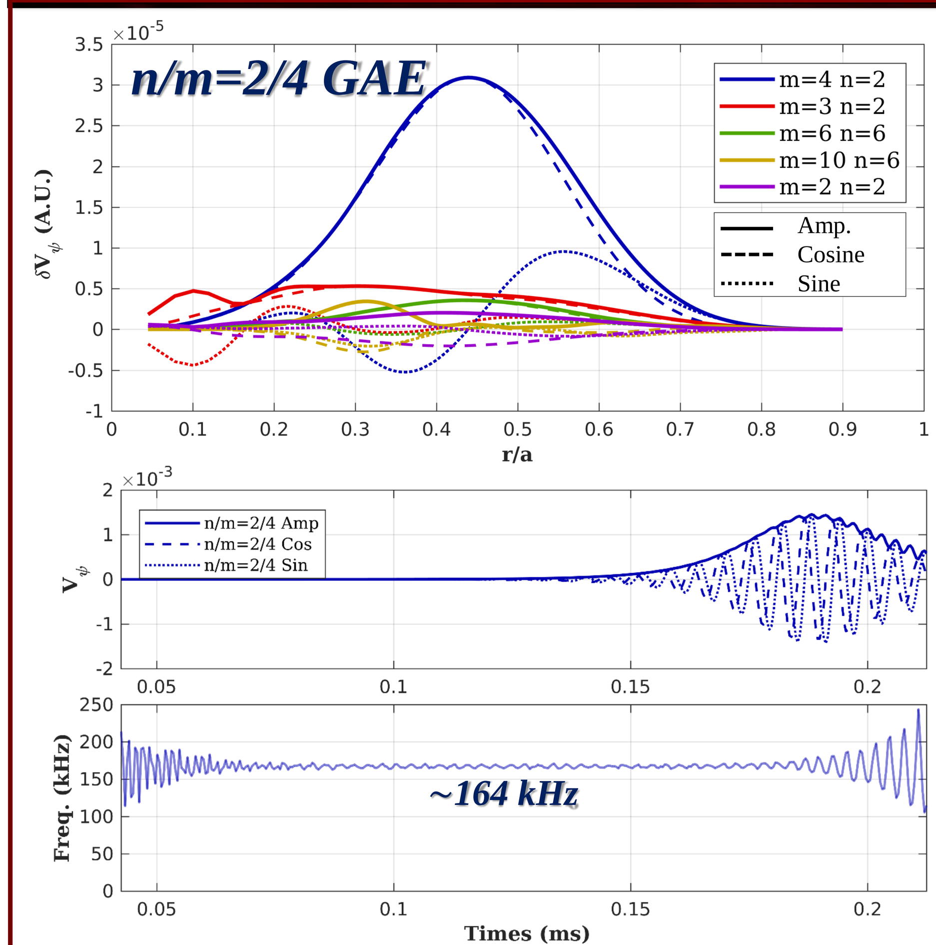

Fig. 6.1: (a) Spatial profile of radial velocity harmonic of |n| = 2 toroidal mode family. Time evolution of (b) amplitude, cosine and sine and (c) frequency of n/m=2/4 radial velocity harmonic

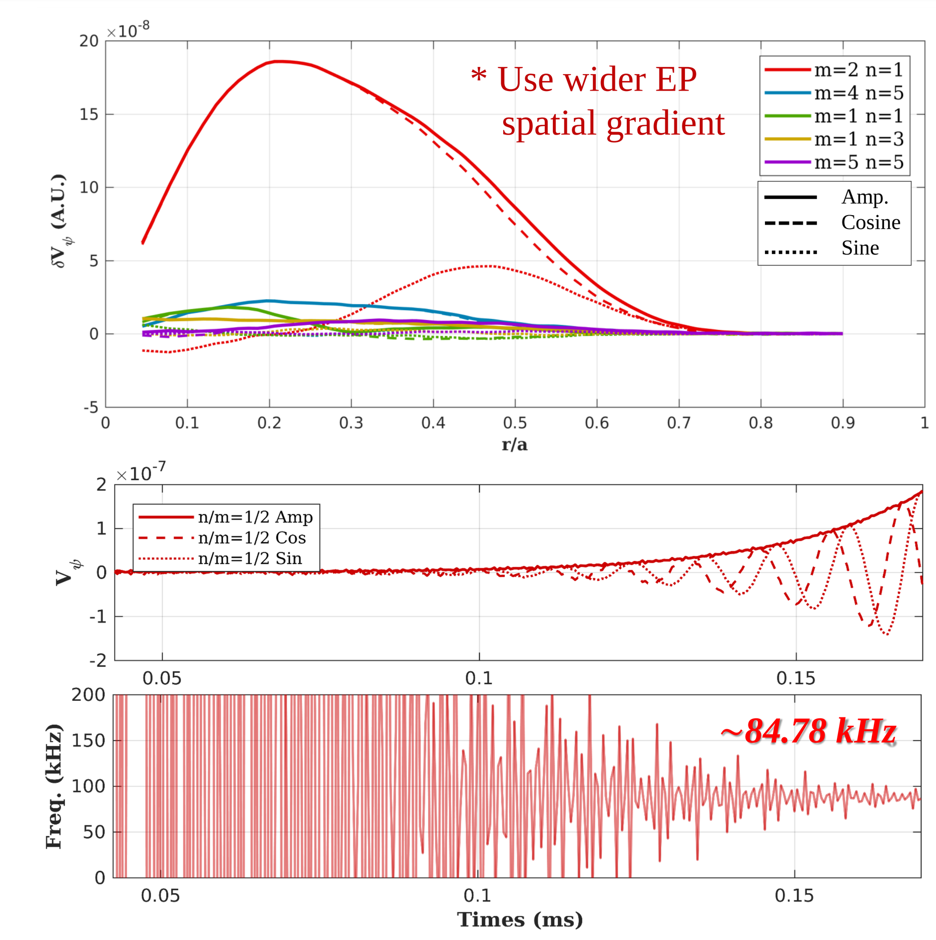

Fig. 6.2: (a) Spatial profile of radial velocity harmonic of |n| = 1 toroidal mode family. Time evolution of (b) amplitude, cosine and sine and (c) frequency of n/m=2/4 radial velocity harmonic

- n/m=2/4 was observed as a **single poloidal dominant mode**.
  → Verify as **Global Alfvén eigenmode.**
  → Validate with experiment and good agreement with the continua.
- |n| = 1 toroidal mode filter is applied to reduce numerical noise.
  → **Significantly lower growth** rate than n/m=2/4 GAE.
  → Localized in the **core region**.
  → Not an experimental observed EPM.

B. Energetic Particle Dynamics :

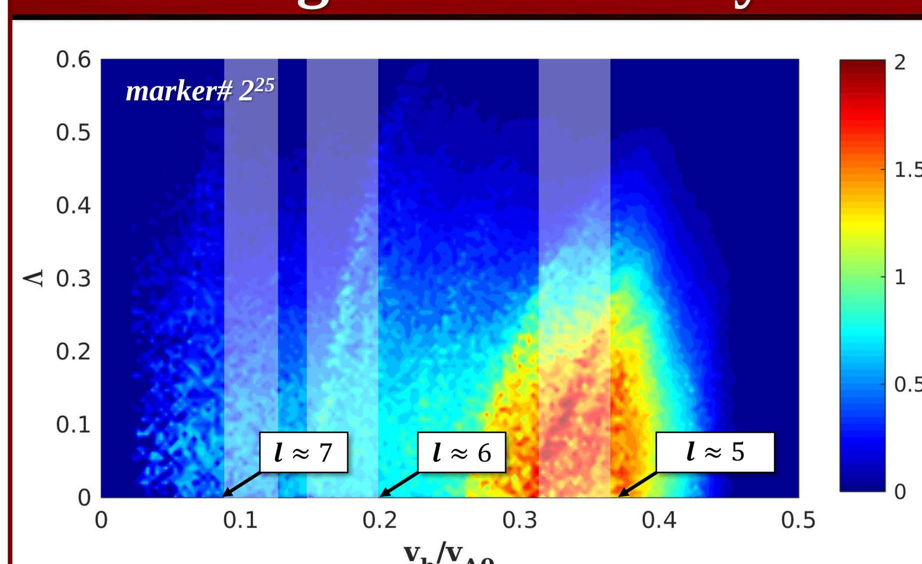

Fig. 6.3: Total Distribution (f) of energetic particle at the saturation point of n/m=2/4 GAE.

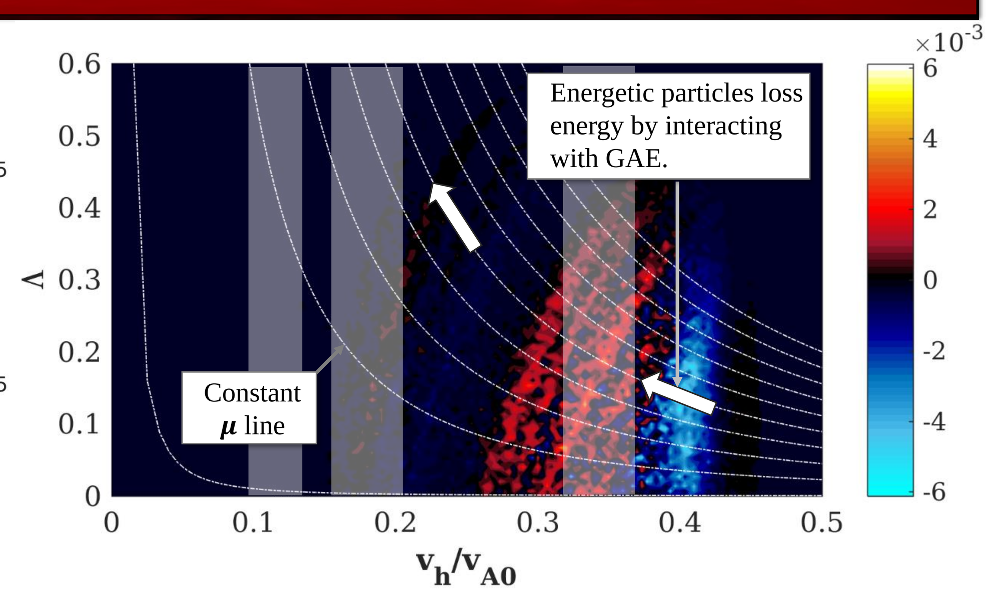

Fig. 6.4: Perturbed distribution (δf) of energetic particle at the saturation point of n/m=2/4 GAE.

- n/m=2/4 GAE is destabilized by energetic particles with velocity of $\mathbf{0.13v_{A0}}$, $\mathbf{0.18v_{A0}}$ and $\mathbf{0.3v_{A0}}$.
  → **Neglect** toroidal mode coupling (j=0)

$$v = \frac{\omega R}{\left(n + jvN_{fp} - \frac{l}{q}\right)} \approx \frac{\omega R}{\left(n - \frac{l}{q}\right)}$$

Mode frequency, Toroidal Mode, EP Toroidal orbit frequency, Poloidal Coupling, EP Poloidal orbit frequency

$$\omega - (n + jvN_{fp})\omega_\phi - l\omega_\theta = 0$$

[5]

Toroidal Mode family coupling

VII.Discussion

- **n/m=2/4 Global Alfvén eigenmode** has been destabilized in nonlinear hybrid simulation model and benchmarked with experimental observation from magnetic probe and density fluctuation signal from BES.
- Global Alfvén eigenmode in Heliotron J was coupled with energetic particle with the energy of $\mathbf{0.13v_{a0}}$, $\mathbf{0.18v_{a0}}$ and $\mathbf{0.3v_{a0}}$ for far passing particle.
  → For passing particle, this energy ranges correspond to drift harmonic ***l*** of **+5**, **+6** and **+7**, respectively, which corresponds to sideband resonance.

VIII. Conclusion & Future Works

- Hybrid simulation code MEGA has been incorporated in Heliotron J configuration.
- **Global Alfvén eigenmode** has been **reproduced** in the simulation, while **energetic particle mode (EPM)** was **not observed**.
  → n/m=1/2 oscillation was observed with low amplitude.
- Toroidal mode coupling effect in Heliotron J (low equilibrium field period) will be studied with filter.
- New methodology will be developed to simulate the Alfvén eigenmode in the peripheral plasma region.
  → Full-f & finite energetic particle pressure in the vacuum region.

IX. References

[1] Y. Todo and T. Sato, Phys. Plasma **5**, 1321 (1998)
[2] S. Yamamoto, et. al, Fusion Science and Technology **51:1**, 92-96 (2007)
[3] S. Yamamoto, et. al, Nuclear Fusion **57**, 126065 (2017)
[4] L.G. Zang, et. al, Nuclear Fusion **59**, 056001 (2019)
[5] M. Kaneko, et. al, Plasmas, Fusion Science and Technology, **50:3**, 428-433 (2005)
[6] Ya. I. Kolesnichenko, et. al, Physics of Plasmas **9**, 517 (2002)